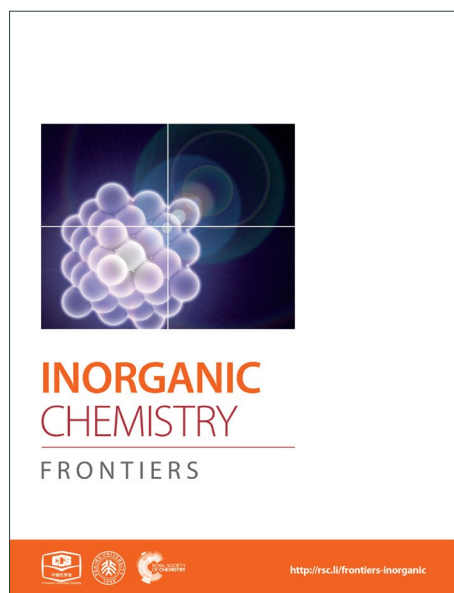
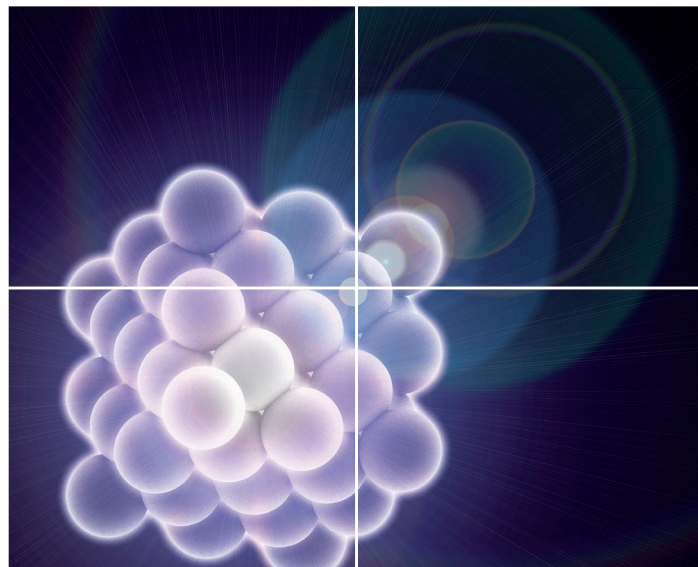


# INORGANIC CHEMISTRY

FRONTIERS

Accepted Manuscript



This is an *Accepted Manuscript*, which has been through the Royal Society of Chemistry peer review process and has been accepted for publication.

*Accepted Manuscripts* are published online shortly after acceptance, before technical editing, formatting and proof reading. Using this free service, authors can make their results available to the community, in citable form, before we publish the edited article. We will replace this *Accepted Manuscript* with the edited and formatted *Advance Article* as soon as it is available.

You can find more information about *Accepted Manuscripts* in the [Information for Authors](#).

Please note that technical editing may introduce minor changes to the text and/or graphics, which may alter content. The journal's standard [Terms & Conditions](#) and the [Ethical guidelines](#) still apply. In no event shall the Royal Society of Chemistry be held responsible for any errors or omissions in this *Accepted Manuscript* or any consequences arising from the use of any information it contains.



Journal Name

ARTICLE

### 3d transition metal complexes with a julolidine–quinoline based ligand: structures, spectroscopies and optical properties

Received 00th January 20xx,  
Accepted 00th January 20xx

DOI: 10.1039/x0xx00000x

www.rsc.org/

Daniel J. Fanna,<sup>a</sup> Yingjie Zhang,<sup>\*b</sup> Li Li,<sup>a</sup> Inna Karatchevtseva,<sup>b</sup> Nicholas D. Shepherd,<sup>a,b</sup> Abdul Azim,<sup>a</sup> Jason R. Price,<sup>c</sup> Janice Aldrich-Wright,<sup>a</sup> Jason K. Reynolds<sup>a</sup> and Feng Li<sup>\*a</sup>

A Schiff base type ligand with the combination of the julolidine and the quinoline groups has been reported as a potential chemosensor in detecting cobalt(II) ion among other heavy and transition metal ions in solution. However, no crystal structure of such ligand with any metal ions has been reported. In this work, its complexation with 3d transition metal ions (Mn(II), Co(II), Ni(II), Cu(II) and Zn(II)) has been investigated with five new complexes being synthesised, spectroscopically and structurally characterised.  $[\text{Mn}_2\text{L}_2(\text{CH}_3\text{OH})_2(\text{CH}_3\text{COO})_2]\cdot\text{CH}_3\text{OH}$  (**1**) (HL ( $\text{C}_{22}\text{H}_{21}\text{N}_3\text{O}$ ) = ((E)-9-((quinolin-8-ylimino)methyl)-1,2,3,5,6,7-hexahydropyrido[3,2,1-ij]quinolin-8-ol)) shows a dinuclear structure with two Mn:L:acetate (1:1:1) units bridged by two methanol molecules.  $[\text{CoL}_2(\text{NO}_3)]\cdot\text{CH}_3\text{OH}\cdot\text{H}_2\text{O}$  (**2**) and  $[\text{NiL}_2]\cdot\text{H}_2\text{O}$  (**3**) exhibit mononuclear structures with Co:L or Ni:L ratio of 1:2.  $[\text{CuL}(\text{CH}_3\text{COO})]\cdot 1/3\text{CH}_3\text{OH}$  (**4**) demonstrates a mononuclear structure and the Cu ion has a square planar coordination polyhedron with a L ligand and a highly non symmetrical acetate anion.  $[\text{Zn}_2\text{L}_2(\text{CH}_3\text{COO})_2]\cdot\text{CH}_3\text{OH}$  (**5**) has two types of dinuclear units, both with two ZnL units bridged by two acetate anions but in three different bridging coordination modes. Their vibrational modes, absorption and photoluminescent properties have also been investigated.

#### Introduction

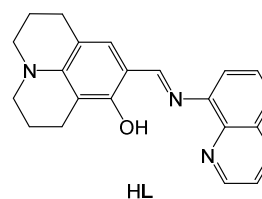
In last decades, colorimetric supramolecular chemistry has attracted considerable attention due to the promise of optical based applications in new technological fields, e.g. chemosensors, fluorescent probes, biomedical imaging, dye-sensitised solar cells, and phase-change optical data storage.<sup>1</sup> The success of these applications is fundamentally reliant on the interactions between colorimetric molecules and external stimulus, such as guest molecules, temperature, pressure, and/or light.<sup>2</sup> Exploration of the systems controlling these interactions is vital for an in-depth understanding into how molecular forces mediate the characteristics within a supramolecular system.<sup>3</sup> Subsequently, this knowledge has potential to be utilised in future syntheses to accurately design a supramolecular system for targeted applications, through directed self-assembly techniques.<sup>4</sup>

The julolidine function group is well known for its visible and fluorescent optical properties, while acting as a strong signal unit.<sup>5</sup> Consequently, it has become a popular functional group in colorimetric studies of metallo-supramolecular

system. The versatility of julolidine has been observed in many chemosensor systems which exhibit selective molecular recognition often for a metal ion<sup>6</sup> or anion.<sup>7</sup> In addition, julolidine has exhibited fluorescent properties in nature which can be explored in the application of fluorescence sensor.<sup>8,9</sup>

Despite strong research effort into julolidine systems, only limited examples of material characterisation involving solid state techniques such as single crystal X-ray diffraction, electron microscopy and vibrational spectroscopy have been utilised.<sup>10</sup>

The Schiff base ligand, HL (see below), consisting of 8-hydroxylulolidine-9-carboxyaldehyde with 8-aminoquinoline, has been reported by Kim and coworkers.<sup>11</sup> Previous studies have demonstrated such ligand has the potential as a Co(II) chemosensor, and a complex of  $\text{CoL}_2$  in solution was confirmed by electron spray ionisation–mass spectroscopy (ESI-MS).<sup>11</sup> However, no crystal structure for any metals with HL is currently available. Clearly there is an urgent need to fill an important niche of structural investigations between solution and solid state studies. More importantly, the structural knowledge will, in turn, provide direct input into the ligand design for future chemosensors towards the potential detection of transition and heavy metal ions.



<sup>a</sup> School of Science and Health, Western Sydney University, Locked Bag 1797, Penrith, NSW 2751, Australia. Email: feng.li@westernsydney.edu.au

<sup>b</sup> Australian Nuclear Science and Technology Organisation, Locked Bag 2001, Kirrawee DC, NSW 2232, Australia. Email: yzx@ansto.gov.au

<sup>c</sup> Australian Synchrotron, 800 Blackburn Road, Clayton, VIC 3168, Australia.

† Electronic Supplementary Information (ESI) available: CCDC 1430317 (**1**), 1438799 (**2**), 14030318 (**3**), 1430319 (**4**) and 1430320 (**5**), 1H NMR, SEM-EDS and ESI-HRMS. See DOI: 10.1039/x0xx00000x

The main focus of this contribution is the structure characterisation and fluorescence properties of the julolidine-quinoline based ligand HL with selected 3d transition metal ions. Herein we report the synthesis, spectroscopies, structures and optical properties of five new complexes of HL with Mn(II), Ni(II), Co(II), Cu(II) and Zn(II) ions in the presence of acetate (OAc) and Co(III) in the presence of nitrate anions for structure only: a dinuclear structure with two Mn(L)(OAc)(CH<sub>3</sub>OH) units bridged by the two methanol molecules for [Mn<sub>2</sub>L<sub>2</sub>(CH<sub>3</sub>OH)<sub>2</sub>(CH<sub>3</sub>COO)<sub>2</sub>·CH<sub>3</sub>OH (**1**); two mononuclear structures with Co:L/Ni:L ratio of 1:2 for [CoL<sub>2</sub>(NO<sub>3</sub>)]·CH<sub>3</sub>OH·H<sub>2</sub>O (**2**) and [NiL<sub>2</sub>]·H<sub>2</sub>O (**3**); a mononuclear structure in the form of Cu(L)(OAc) for [CuL(CH<sub>3</sub>COO)]·1/3CH<sub>3</sub>OH (**4**); and two types of dinuclear units, both with pairs of Zn(L)(OAc) units bridged by the two acetate anions but in three different bridging coordination modes for [Zn<sub>2</sub>L<sub>2</sub>(CH<sub>3</sub>COO)<sub>2</sub>·CH<sub>3</sub>OH (**5**).

## Experimental section

### Materials

All reagents were purchased from commercial sources and used without further purification.

### Physical measurements

The <sup>1</sup>H NMR spectrum was recorded on a Bruker 300 MHz spectrometer. Scanning electron microscope – electron dispersive spectroscopy (SEM-EDS) was conducted using a Zeiss Ultra Plus SEM (Carl Zeiss NTS GmbH, Oberkochen, Germany) under an accelerating voltage of 20 kV. Electrospray ionisation high resolution mass spectroscopy (ESI-HRMS) analysis was conducted utilising a Waters Xevo QToF/nanoaquity UPLC in positive ion mode. Raman spectra were recorded on a Bruker Senterra using the OPUS software and excitation laser 785 nm in the range of 2,000–100 cm<sup>-1</sup>. Absorption spectra were collected using an Agilent Cary 100 spectrophotometer. Fluorescent emission measurements were conducted on a Shimadzu RF-5301PC instrument with a Xenon lamp and excitation wavelength of 470 nm. Solid state fluorescent emission spectra were measured on an Olympus FluoView™ FV1000 Confocal Laser Scanning Microscope, with an external Argon Ion laser (488 nm).

### Ligand synthesis

The synthesis of ligand (HL) involved Schiff base condensations using an optimisation of a literature method.<sup>11</sup> 8-hydroxyjulolidine-9-carboxaldehyde (500 mg, 2.3 mmol) was dissolved in 15 mL acetonitrile. To this solution, an acetonitrile solution of 8-aminoquinoline (330 mg, 2.3 mmol) in 15 mL was added drop wise. After that, a few milligrams of *p*-toluenesulfonic acid was added as a catalyst. This reaction was conducted at reflux condition under nitrogen atmosphere for 18 hours. Once reflux had concluded, the solution underwent a hot filtration to remove any solid impurities. The filtrate was left to evaporate, additional CH<sub>3</sub>CN added and a yellow precipitate collected. This process was repeated three times, with an approximately 60% yield. <sup>1</sup>H NMR (300 MHz, CDCl<sub>3</sub>): δ

9.01 (q, 1H), 8.36 (s, 1H), 8.13 (q, 1H), 7.54 (d, 3H), 7.44 (q, 1H), 6.74 (s, 1H), 3.26(t, 4H, julolidine - aliphatic ring), 3.85 (t, 2H, julolidine - aliphatic ring), 2.65 (t, 2H, julolidine - aliphatic ring), 1.95 (m, 4H, julolidine - aliphatic ring). ESI-HRMS (positive-ion detection, MeOH): *m/z* = 344.1767 (calc. 344.1763 for [HL+H]<sup>+</sup>).

### Complex synthesis

The complexation of HL with Mn(II), Co(II), Ni(II), Cu(II) and Zn(II) ions was carried out using metal acetates. As the procedures of preparing the five complexes are essentially the same, the general preparation of complexes **1-5** is detailed below.

HL (100 mg, 0.29 mmol) was dissolved in 15 mL of methanol. The required metal (Mn(II), Co(II) Ni(II), Cu(II) and Zn(II)) acetates (0.145 mmol) in 15 mL of methanol was slowly added to the above ligand solution. The mixture was then heated at 70°C for 90 minutes. Hot filtration was immediately conducted to remove any solid impurities. The product of **1-5** was obtained by slow evaporation. The single crystals of **1, 3-5** used for X-ray crystallography were obtained by slow diffusion of diethyl ether vapour into the resulting complexes in MeOH. Unfortunately, the single crystal of complex **2** in acetate form can't be obtained, although several crystallisation methods have been performed. While a single crystal of **2** was successfully obtained using Co(II) nitrate instead of acetate with the addition of triethylamine for deprotonation of HL.

**1**: Yield: 62%. UV/Vis (MeOH): λ<sub>max</sub>/nm = 468, Raman (solid state, Laser = 785 nm): 1563, 1494, 1467, 1371, 1302, 1224, 1090, 807 cm<sup>-1</sup>. ESI-HRMS (positive-ion detection, MeOH): *m/z* = 739.2599 (calc. 739.2593 for [MnL<sub>2</sub>]<sup>+</sup>); 397.1007 (calc. 397.0987 for [MnL]<sup>+</sup>);

**2**: Yield: 40%. UV/Vis (MeOH): λ<sub>max</sub>/nm = 495, Raman (solid state, Laser = 785 nm): 1615, 1563, 1493, 1467, 1371, 1302, 1220, 1090, 520, cm<sup>-1</sup>; ESI-HRMS (positive-ion detection, MeOH): *m/z* = 743.2559 (calc. 743.2545 for [CoL<sub>2</sub>]<sup>+</sup>); 401.0951 (calc. 401.0938 for [CoL]<sup>+</sup>);

**3**: Yield: 73%. UV/Vis (MeOH): λ<sub>max</sub>/nm = 480, Raman (solid state, Laser = 785 nm): 1617, 1564, 1490, 1463, 1418, 1372, 1298, 1264, 1233, 1088, 1020, 960, 803, 502 cm<sup>-1</sup>. ESI-HRMS (positive-ion detection, MeOH): *m/z* = 743.2646 (calc. 743.2644 for [NiL<sub>2</sub>+H]<sup>+</sup>); 400.0950 (calc. 400.0960 for [NiL]<sup>+</sup>);

**4**: Yield: 46%. UV/Vis (MeOH): λ<sub>max</sub>/nm = 468, Raman (solid state, Laser = 785 nm): 1567, 1494, 1467, 1376, 1320, 1298, 1273, 1232, 1093, 1027, 961, 807, 519, 490 cm<sup>-1</sup>. ESI-HRMS (positive-ion detection, MeOH): *m/z* = 405.0913 (calc. 405.0902 for [CuL]<sup>+</sup>);

**5**: Yield: 66%. UV/Vis (MeOH): λ<sub>max</sub>/nm = 468, Raman (solid state, Laser = 785 nm): 1565, 1494, 1466, 1428, 1373, 1301, 1236, 1091, 1065, 969, 896, 829, 806, 635, 505, 442, 316 cm<sup>-1</sup>. ESI-HRMS (positive-ion detection, MeOH): *m/z* = 406.0902 (calc. 406.0898 for [ZnL]<sup>+</sup>).

### Single crystal X-ray diffraction

The single crystal X-ray diffraction measurements for complexes **1-5** were carried out on the MX1 beamline at the Australian Synchrotron. Diffraction data were collected using

**Table 1.** Crystal data and refinement details for complexes 1-5.

Complex	1	2	3	4	5
Formula	C <sub>50</sub> H <sub>53</sub> N <sub>6</sub> O <sub>9</sub> Mn <sub>2</sub>	C <sub>45</sub> H <sub>44</sub> N <sub>7</sub> O <sub>6</sub> Co	C <sub>44</sub> H <sub>42</sub> N <sub>6</sub> O <sub>3</sub> Ni	C <sub>73</sub> H <sub>73</sub> N <sub>9</sub> O <sub>10</sub> Cu <sub>3</sub>	C <sub>49</sub> H <sub>50</sub> N <sub>6</sub> O <sub>7</sub> Zn <sub>2</sub>
Formula weight	991.86	837.80	761.54	1427.02	965.73
Crystal system	monoclinic	monoclinic	monoclinic	monoclinic	triclinic
Space group	<i>P</i> 2 <sub>1</sub> / <i>n</i>	<i>P</i> 2 <sub>1</sub> / <i>n</i>	<i>C</i> 2/ <i>c</i>	<i>P</i> 2 <sub>1</sub> / <i>c</i>	<i>P</i> -1
<i>a</i> (Å)	10.460(2)	21.900(4)	20.534(4)	8.9270(18)	12.804(3)
<i>b</i> (Å)	12.325(2)	18.010(4)	13.565(3)	23.859(5)	17.462(3)
<i>c</i> (Å)	18.253(4)	23.630(5)	15.695(3)	29.072(6)	19.515(4)
$\alpha$ (°)	90	90	90	90	87.20(3)
$\beta$ (°)	94.73(3)	101.89(3)	125.65(3)	98.29(3)	88.48(3)
$\gamma$ (°)	90	90	90	90	89.90(3)
Volume (Å <sup>3</sup> )	2345.2(8)	9120(3)	3552.3(16)	6127(2)	4356.5(15)
<i>Z</i> / $\mu$ (mm <sup>-1</sup> )	2 / 0.602	8 / 0.429	4 / 0.599	4 / 1.105	4 / 1.162
Min./Max. $\theta$ [°]	2.239/30.164	1.155/27.924	2.005/27.914	1.653/25.499	1.045/30.069
<i>d</i> <sub>calcd</sub> (g cm <sup>-3</sup> )	1.405	1.220	1.424	1.547	1.472
<i>GOF</i>	1.038	1.104	1.082	1.075	1.085
Final <i>R</i> <sub>1</sub> <sup>a</sup> [ <i>I</i> > 2 $\sigma$ ( <i>I</i> )]	0.0638	0.0808	0.0340	0.0763	0.0620
Final <i>wR</i> <sub>2</sub> <sup>b</sup> [ <i>I</i> > 2 $\sigma$ ( <i>I</i> )]	0.1797	0.2523	0.0859	0.2068	0.1658

$$^a R_1 = \frac{\sum ||F_o| - |F_c||}{\sum |F_o|} \quad ^b wR_2 = \left\{ \frac{\sum [w(F_o^2 - F_c^2)]^2}{\sum [w(F_o^2)]^2} \right\}^{1/2}$$

Si<111> monochromated synchrotron X-ray radiation ( $\lambda = 0.71074$ ) at 100(2) K with Bluelce software<sup>12</sup> and were corrected for Lorentz and polarization effects using the XDS software.<sup>13</sup> An empirical absorption correction was then applied using SADABS.<sup>14</sup> The structures were solved by direct methods and the full-matrix least-squares refinements were carried out using a suite of SHELX program<sup>15</sup> via Olex<sup>2</sup> interface.<sup>16</sup> All non-hydrogen atoms were located from the electron density maps and refined anisotropically. Hydrogen atoms bound to carbon atoms were added in the ideal positions and refined using a riding model. The refinement of **4** revealed that one (Cu3) of the three distinguished monomeric units has a carbon atom at the julolidine side disordered in two equal positions. In addition, the carboxylate O atom occupying one of the square positions deviates from the plane. Consequently, the relatively higher negative residue density at Cu3 causes several alerts at B level. Furthermore, the data completeness for **4** is a bit low due to its crystallization in low symmetry space group and the crystal suffered gradual radiation damage which only allows one circle data collection possible. All potential hydrogen bonds were calculated using PLATON.<sup>17</sup>

## Results and discussion

### Synthesis and characterization

Ligand HL was prepared by optimising a literature procedure.<sup>11</sup> <sup>1</sup>H NMR spectrum (Fig. S1, ESI<sup>+</sup>) and electrospray ionization high resolution mass spectrometry (ESI-HRMS) (Fig. S2, ESI<sup>+</sup>) results were consistent with the proposed structure of HL. Complexes **1-5** were prepared by reactions of metal acetates and HL in methanol with a ratio of 1:2. Although the extra ligand has been applied for all

reactions, only Ni(II) and Co(III) complexes can be obtained in the formula of ML<sub>2</sub> in solid state. In solution, ESI-HRMS results (Figs. S3, 6, 9, 12 and 14, ESI<sup>+</sup>) easily revealed major peaks of ML<sub>2</sub> for complexes **1**, **2** and **3**, and ML for complexes **3**, **4** and **5**. A few minor fragments of ML for **1** and **2** were also identified (Figs. S3 and 6, ESI<sup>+</sup>). The appropriate isotope patterns for their complexes were observed (Figs. S4, 5, 7, 8, 10, 11, 13 and 15, ESI<sup>+</sup>) and the isotopic distributions for ML or ML<sub>2</sub> are in great agreement with their calculated patterns. In addition, SEM-EDS analysis confirmed the presence of C, N, O and Mn in **1**; C, N, O, Co in **2**; C, N, O and Ni in **3**; C, N, O, Cu in **4**; and C, N, O, Zn in **5** (Figs. S16–S20, ESI<sup>+</sup>).

### Structure description and discussion

The crystal data and refinement details for complexes **1-5** are summarized in Table 1 and selected bond lengths of the metal coordination polyhedron are listed in Table 2. The asymmetric unit of **1** contains a Mn(II) ion coordinated by a tridentate L ligand, a monodentate acetate and a methanol molecule. The expansion by symmetry suggests that the structure of **1** is constructed with two Mn(L)(OAc) units linked by two bridging methanol molecules forming a dinuclear complex (Fig. 1a). The Mn(II) ion is six-fold coordinated with a chelating L [2.051(2) Å for Mn1–N1, 1.999(2) Å for Mn1–N2 and 1.881(2) Å for Mn1–O1], a monodentate acetate [2.182(2) Å for Mn1–O2] and two bridging methanol molecules [1.896(2) and 2.258(2) Å for Mn1–O4 and Mn1–O4'] making a slightly distorted octahedral coordination environment for the Mn metal centre. The Mn–Mn distance within the dinuclear complex is 3.222(1) Å. The L ligand adopts fairly flat conformation (Fig. 1b). Strong  $\pi$ – $\pi$  interactions between dinuclear units (Fig. 1b) lead to the formation of one dimensional (1D) columns along the crystallographic *c*-axis (Fig. 1c). The free terminal carboxylate

**Table 2.** Selected bond lengths of metal coordination polyhedron in 1-5.

<b>1</b>			
Mn1–O1	1.881(2)	Mn1–N1	2.051(2)
Mn1–N2	1.999(2)	Mn1–O2	2.182(2)
Mn1–O4	1.896(2)	Mn1–O4'	2.258(2)
<b>2</b>			
Co1–O1	1.881(2)	Co1–N1	1.946(3)
Co1–N2	1.904(3)	Co1–O2	1.874(2)
Co1–N4	1.935(3)	Co1–N5	1.907(3)
Co2–O3	1.878(2)	Co2–N7	1.940(3)
Co2–N8	1.905(3)	Co2–O4	1.879(2)
Co2–N10	1.941(3)	Co2–N11	1.900(3)
<b>3</b>			
Ni1–O1	2.028(2)	Ni1–N1	2.094(2)
Ni1–N2	2.021(2)		
<b>4</b>			
Cu1–O1	1.895(3)	Cu1–N1	1.985(4)
Cu1–N2	1.944(4)	Cu1–O2	1.948(3)
Cu1–O3	2.678(4)	Cu2–O4	1.896(3)
Cu2–N4	1.999(3)	Cu2–N5	1.939(4)
Cu2–O5	1.950(4)	Cu2–O6	2.763(3)
Cu3–O7	1.842(4)	Cu3–N7	1.992(4)
Cu3–N8	1.977(4)	Cu3–O8	1.962(4)
Cu3–O9	2.677(4)		
<b>5</b>			
Zn1A–O1A	1.974(2)	Zn1A–N1A	2.134(3)
Zn1A–N2A	2.052(2)	Zn1A–O1AA	2.070(2)
Zn1A–O1BB	2.108(2)	Zn1B–O1B	2.007(2)
Zn1B–N1B	2.181(3)	Zn1B–N2B	2.042(2)
Zn1C–O1C	1.998(2)	Zn1C–N1C	2.185(3)
Zn1C–N2C	2.030(2)	Zn1C–O2CC	2.011(2)
Zn1C–O1DD	2.007(2)	Zn1D–O1D	1.988(2)
Zn1D–N1D	2.150(3)	Zn1D–N2D	2.060(3)

**Table 3.** Calculated hydrogen bonds for complexes 1-5.

Donor–H...Acceptor	<i>d</i> (D–H)	<i>d</i> (H...A)	<i>d</i> (D...A)	∠(DHA)
<b>1</b>				
O5–H5A...O3	0.82	2.16	2.682(8)	122
<b>2</b>				
O1A–H1A...O1B3	0.82	2.54	2.8221	102
O2A–H2A...O2B2	0.82	2.18	2.7902	132
<b>3</b>				
O1W–H1W...O1	0.89	2.03	2.820(2)	149
<b>4</b>				
O1S–H1S...O6	0.82	1.90	2.719(7)	176
<b>5</b>				
O1S–H1S...O2CC	0.82	1.91	2.725(4)	170
O2S–H2S...O2BB	0.82	1.90	2.717(4)	173

O atom of the acetate anion is involved in hydrogen bonding with the lattice methanol molecule (Table 3).

Complex **2** has two 1:2 monomeric structures (Fig. 2a, b) in the asymmetric unit with two Co(III) ions each six-fold coordinated by two L ligands [1.946(3) Å for Co1–N1, 1.904(3) Å for Co1–N2 and 1.881(2) Å for Co1–O1; 1.935(3) Å for Co1–N4, 1.907(3) Å for Co1–N5 and 1.874(2) Å for Co1–O2; 1.940(3) Å for Co2–N7, 1.905(3) Å for Co2–N8 and 1.878(2) Å for Co2–O3; 1.941(3) Å for Co2–N10, 1.900(3) Å for Co2–N11

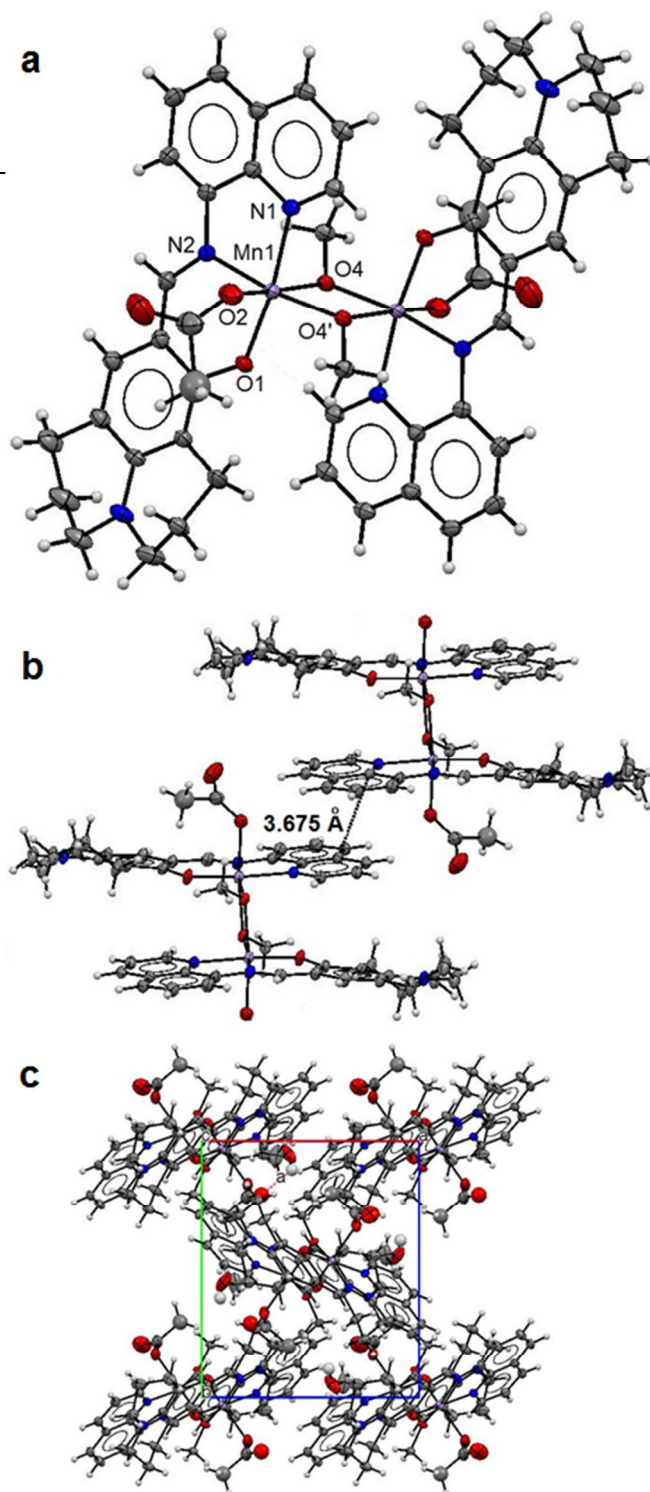


**Fig. 1.** Structure of **1**: An ellipsoidal plot (50% probability) of the dinuclear structure (a),  $\pi$ - $\pi$  interactions between dimer units (b) and a crystal packing view along the *c*-axis (c).

and 1.879(2) Å for Co2–O4] making octahedral coordination environments for the Co metal centres. The L ligands have fairly flat conformations leading to parallel packing in the crystal lattice (Fig. 2c). The lattice methanol molecules and

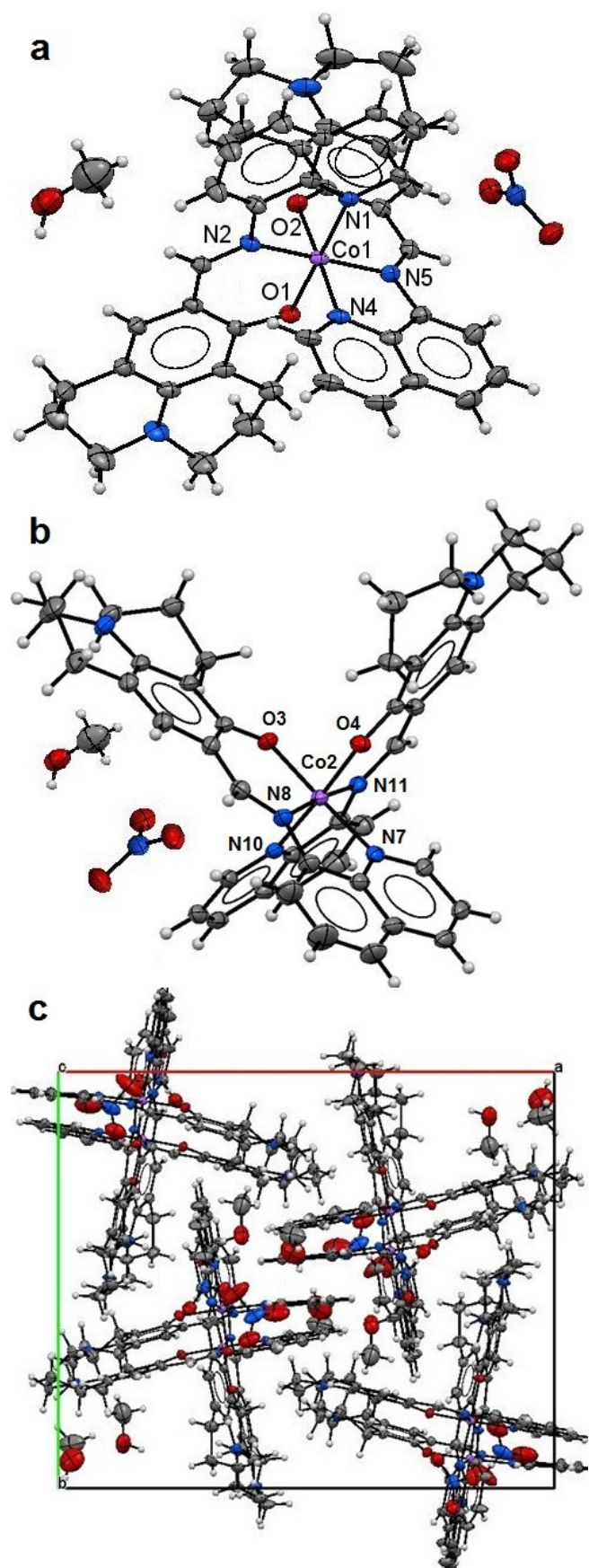


Fig. 2. Structure of **2**: The ellipsoidal plots (50% probability) of the mononuclear structures (a, b) and a crystal packing along the *c*-axis (c).

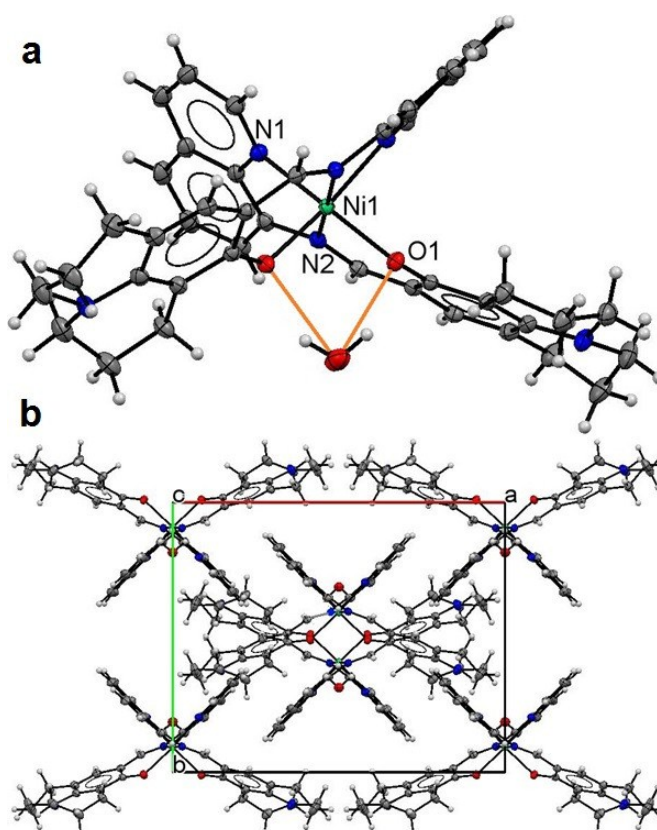


Fig. 3. Structure of **3**: An ellipsoidal plot (50% probability) of the mononuclear structure (a) with hydrogen bonds in orange and a crystal packing along the *c*-axis (b).

nitrate anions are involved in hydrogen bonding (Table 3). Although Kim and co-workers<sup>11</sup> have reported the preparation of ligand (HL) and its use as a Co(II) chemosensor, no X-ray structure of the corresponding cobalt complex was presented. In their studies, the majority of the evidence suggested that the complex was a Co(II) species, the ESI-MS result was in conflict with this in that it was in accord with the presence of Co(III). In this study, the Co(III) structure determined indicates that the aerial oxidation of the initial cobalt(II) complex formed in solution does happen during the crystallization process which started in 10 hours.

The asymmetric unit of **3** has half of a Ni(II) ion on a centre symmetry coordinated by a tridentate L ligand with half a lattice water molecules. The expansion by symmetry suggests that **3** has a 1:2 monomeric structure (Fig. 3a) with a Ni(II) ion six-fold coordinated by two L ligands [2.028(2) Å for Ni1–N1, 2.094(2) Å for Ni1–N2 and 2.028(2) Å for Ni1–O1] making an octahedral coordination environment for the Ni metal centre. The L ligand has slightly twisted boat conformation (Fig. 3a). The lattice water molecule has hydrogen bonding with both L ligands (O1 and O1#) (Fig. 2a) (Table 3). The monomers in the butterfly shape are packed in the crystal lattice (Fig. 3b).

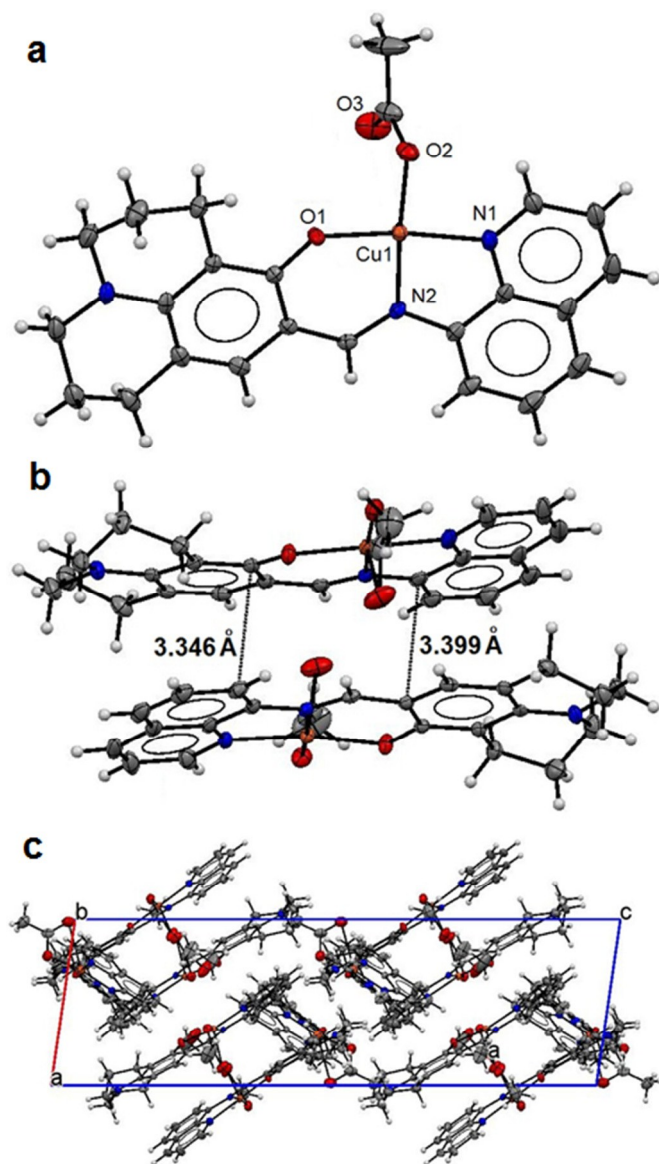


Fig. 4. Structure of **4**: An ellipsoidal plot (50% probability) of the mononuclear structure (a),  $\pi$ - $\pi$  interactions between monomers (b) and a crystal packing view along the  $c$ -axis (c).

The asymmetric unit of **4** contains three distinguished monomeric structures, each was made up of a Cu(II) ion five-fold coordinated by a **L** ligand [1.985(4) to 1.999(3) Å for Cu–N1/N4/N7; 1.939(4) to 1.977(4) Å for Cu–N2/N5/N8 and 1.842(4) to 1.896(3) Å for Cu–O1/O4/O7] and a chelating acetate anion [1.948(4) to 1.962(3) Å Cu–O2/O5/O8 and 2.677(4) to 2.763(3) Å Cu–O3/O6/O9] making square planar coordination polyhedra for the Cu metal centres (Fig. 4a) as Cu–O3/O6/O9 weak bonding represents an intermediate coordination mode of acetate between mono- and bidentate. Extensive  $\pi$ - $\pi$  interactions (Fig. 4b) between monomers lead to the parallel crystal packing in the crystal lattice (Fig. 4c). A free terminal carboxylate O atom (O6) from one of the acetate anions is involved in hydrogen bonding with the lattice methanol molecule (Table 3).

The structure of **5** is composed of two dinuclear units (Fig. 5a, b) in the asymmetric unit. Each dimer unit has two pairs

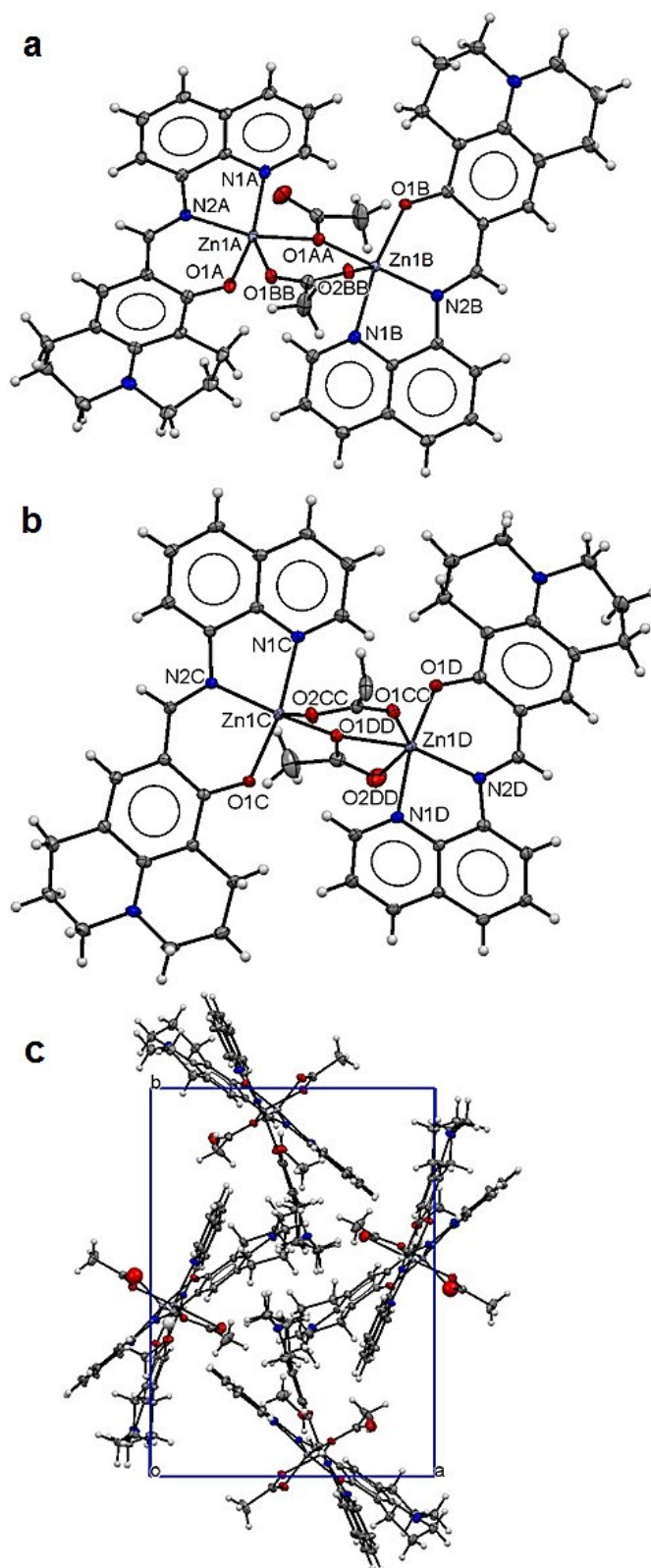


Fig. 5. Structure of **5**: Ellipsoidal plots (50% probability) of dinuclear unit 1 (a), unit 2 (b) and a crystal packing view along the  $c$ -axis (c).

of ZnL units bridged by two acetate anions. In the dimer unit 1 (Fig. 5a), both Zn(II) ions are five-fold coordinated with a chelating **L** [2.134(3) Å for Zn1A–N1A, 2.052(3) Å for Zn1A–N2A, 1.974(3) Å for Zn1A–O1A; 2.181(3) Å for Zn1B–N1B, 2.042(3) Å for Zn1B–N2B, 2.007(2) Å for

Zn1B–O1B] and two bridging acetates [2.070(2) Å for Zn1A–O1AA, 2.108(2) Å for Zn1A–O1BB; 2.014(2) Å for Zn1B–O1AA, 2.022(2) Å for Zn1B–O2BB] making slightly distorted trigonal bipyramidal coordination environments for both Zn metal centres. The two bridging acetate anions adopt different coordination modes: one bridges through only one carboxylate O and the other bridges through both carboxylate O atoms in the *cis*- arrangement. In the case of dimer unit 2 (Fig. 5b), both Zn(II) ions are coordinated with one chelating L [2.185(3) Å for Zn1C–N1C, 2.030(3) Å for Zn1C–N2C, 1.998(2) Å for Zn1C–O1C; 2.150(3) Å for Zn1D–N1D, 2.060(3) Å for Zn1D–N2D, 1.988(2) Å for Zn1D–O1D] and two bridging acetates [2.007(2) Å for Zn1C–O1DD, 2.011(2) Å for Zn1C–O2CC; 2.129(2) Å for Zn1D–O1CC, 2.120(2) Å for Zn1D–O1DD, 2.480(2) Å for Zn1D–O2DD]. Again the two acetate anions have different coordination modes: one bridges through both carboxylate O atoms in the *cis*- arrangement whilst the other one chelates to one metal centre and then bridges to the other via one carboxylate O atom making five-fold coordination of Zn1C in a trigonal bipyramidal polyhedron and six-fold coordination of Zn1D in octahedral polyhedron. The Zn–Zn distances within the dimer units range from 3.625(4) Å for Zn1A–Zn1B to 3.701(4) Å for Zn1C–Zn1D. The L ligands adopt very flat conformations (Fig. 5c) leading to isolated dimers packing along the crystallographic *c*-axis (Fig. 5c). Carboxylate O atoms (O2BB and O2CC) are involved in hydrogen bonding with the lattice methanol molecules (Table 3).

Three structural types, e.g. 1:1 monomer (**4**); 1:2 monomer (**2** and **3**); 2:2 dimer (**1** and **5**) have been identified in this study. The coordination of HL to Cu(II) produced a square planar polyhedron in **4** where a tridentate L and an acetate anion were bound to the metal centre with the acetate in a highly non symmetrical fashion. It is interesting to observe one normal carboxylate O bonding to Cu(II) ion with average bond length of 1.951(3) Å for Cu1–O2/O5/O8 whilst the other with much longer average Cu–O bond, average 2.704(3) Å for Cu1–O3/O6/O9. This represents an intermediate coordination mode between mono- and bidentate with the second oxygen atom weakly interacting with the metal centre. Such acetate bonding to Cu(II) ion has been observed in early studies.<sup>18</sup> The mononuclear structure with metal to ligand ratio of 1:2 exhibiting an octahedral coordination geometry was found for both Co(III) in **2** and Ni(II) in **3**. In the literature, many complexes of Mn(II), Fe(II)/(III), Co(II)/(III), Ni(II) and Zn(II) ions with Schiff base ligands in the similar tridentate (N, N, O) geometry result in similar 1:2 complexes due to the preferred metal octahedral coordination polyhedra.<sup>19</sup> Although Mn(II) ions in **1** also adopt octahedral coordination geometry, its structure was not consistent with that observed for Co(III) and Ni(III). Instead, two MnL(OAc) units were bridged together by two methanol molecules forming a dimer with two monodentate acetate anions. This dimer structure was quite unique not only because a 1:2 coordination arrangement was not formed but also due to the fact that the dimer was bridged

through methanol molecules. A slightly different dimer structure has been identified in **5** with acetate anions bridging in three different coordination modes. In fact, the acetate anions are present as monodentate in **1** and **4**, and bridging in **5**. It is apparent that the crystal structures obtained in this study have been controlled by two main factors. One is the metal preferred coordination geometry and the other is the competition of additional ligands, e.g. acetate anion and methanol solvent in the case of **1** and **5**. It is also observed that the L ligand can adopt flexible, from fairly flat (**1**, **2**, **4** and **5**) to bending (**3**) conformations. The flat ligand conformations present in **1**, **2**, **4** and **5** lead to closely parallel packing of ligands in the crystal lattice. Consequently,  $\pi$ - $\pi$  interactions are very common in their crystal structures.

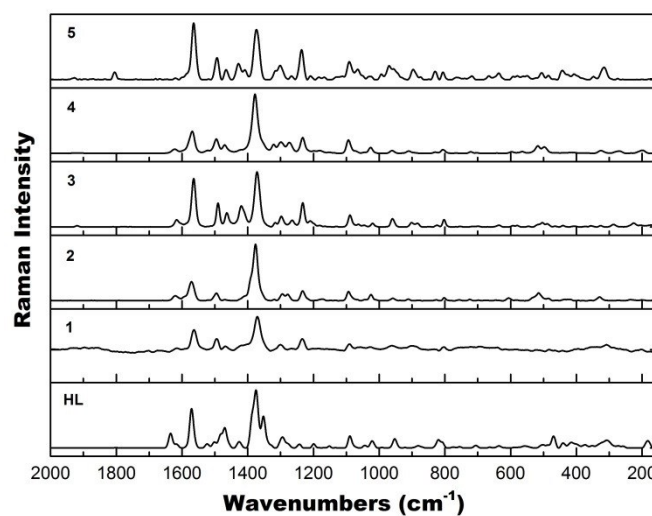


Fig. 6. Raman spectra of HL and 1-5 in 2,000-200  $\text{cm}^{-1}$  region.

#### Raman spectroscopy

The vibrational modes of the five complexes have been examined using Raman spectroscopy. All Raman spectra of complexes **1-5** (Fig. 6) resemble each other quite well and are similar to the Raman spectrum of HL (Fig. 6) due to the presence of the same ligand. Common features mainly from quinoline functional group<sup>20</sup> include:  $\nu(\text{C}=\text{C})$  at 1564  $\text{cm}^{-1}$ ;  $\nu(\text{C}=\text{N})$  at 1494  $\text{cm}^{-1}$ ;  $\nu(\text{CC}) + \nu(\text{CN})$  at 1466 and 1321–1300  $\text{cm}^{-1}$ ;  $\nu(\text{C}-\text{C})$  at 1370  $\text{cm}^{-1}$ ;  $\nu(\text{C}-\text{N}) + \delta(\text{CH})$ , in-plane bending at 1234  $\text{cm}^{-1}$ ;  $\delta(\text{CH})$ , in-plane bending +  $\delta(\text{CNC})$  at 1093  $\text{cm}^{-1}$ ;  $\nu(\text{CNCH})$  at 965  $\text{cm}^{-1}$ ;  $\delta(\text{CH})$ , out-of-plane bending +  $\delta(\text{CCC}) + \delta(\text{CCN})$  at 806  $\text{cm}^{-1}$ .

#### Absorption and photoluminescence

The absorption spectra of the five metal acetates [Mn(II), Co(II), Ni(II), Cu(II) and Zn(II)] and HL in methanol solutions with metal to ligand ratio of 1:2 are shown in Figure 7. HL gives double absorption maxima at  $\sim 435$  and  $\sim 445$  nm and the corresponding complexes have the absorption maxima slightly shifted to  $\sim 468$  nm upon complexation, with further shift to  $\sim 480$  nm for **3**. Co(III) ion gives very similar absorption

spectrum to that of Ni(II) but with a bit further shift towards ~495 nm, consistent with the earlier observation.<sup>11</sup> After excitation at 470 nm, HL and 1-4 have the fluorescence emission maxima at ~560 nm with the exception of 5 which has the fluorescence emission maxima shifted to ~575 nm. (Fig. 7). It is also evident that Mn(II) ion in 1, Co(III) ion in 2, Ni(II) ion in 3 and Cu(II) ion in 4 quench the ligand fluorescence emissions whilst Zn(II) ion in 5 has enhanced the ligand fluorescence emission. It has been well documented that paramagnetic metal ions quench fluorescence in systems of the present type. On the other hand, Zn(II) with its full-shell electronic configuration ( $d^{10}$ ) does not profit from ligand field effects. In addition, Zn(II) ion is photophysically inactive, as it does not display any one-electron redox activity and cannot be involved in electronic transfer process. However, Zn(II) ion can exert an indirect effect on the emitting activity of a proximate fluorophore, which may lead to fluorescence regeneration or enhancement<sup>21</sup>, as observed in the present study.

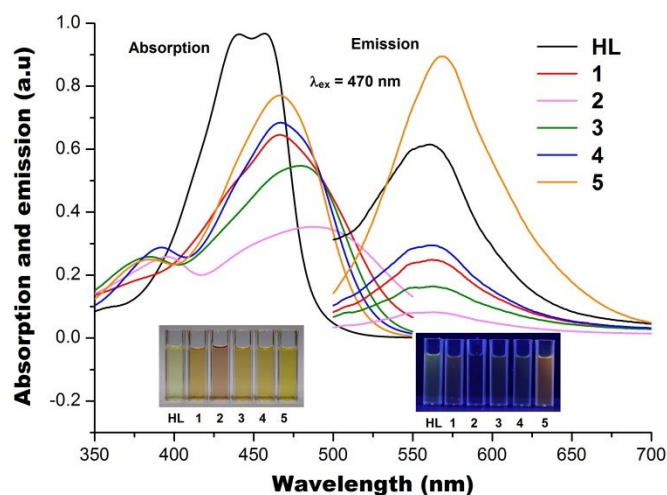


Fig. 7. The absorption and emission spectra of HL and 1-5 in methanol solutions.

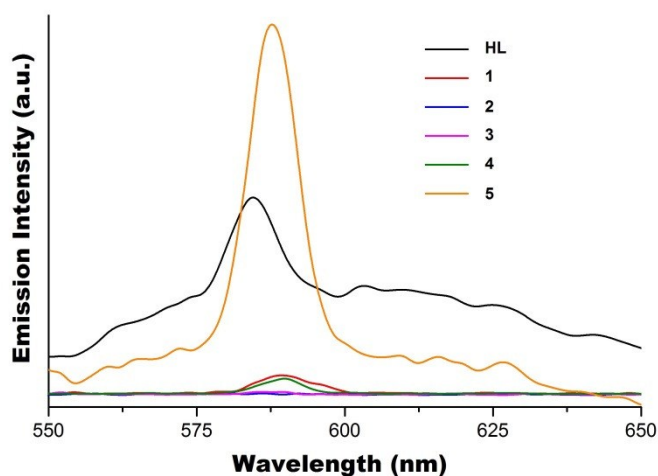


Fig. 8. The emission spectra of HL, and complexes 1-5 in solid state.

The solid state fluorescence emission spectra of complexes 1-5 together with ligand HL are shown in Figure 8. Similar to the observation from the solution study, the fluorescence of HL is completely quenched in complexes 2 and 3 which have the metal to ligand ratio of 1:2, and partially quenched in complexes 1 and 4 which have the metal to ligand ratio of 1:1, with emission maxima at ~588 nm. As expected, the enhancement of solid state fluorescence emission of HL by the presence of Zn(II) in 5 is obvious with the emission maximum shifted to ~588 nm compared to ~585 nm for ligand HL.

## Conclusions

Five new complexes with structures ranging from monomers with metal to ligand ratios of 1:1 and 1:2 to dimers bridged by either acetate anions or methanol molecules have been synthesised and characterised. Octahedral coordination geometry is favored in Mn(II), Co(III) and Ni(II) complexes with a dimer structure for Mn(II) via unique methanol instead of acetate bridging. Co(III) and Ni(II) ions adopt mononuclear structures with metal to ligand ratio of 1:2 with flat ligand conformation for Co(III) complex and twisted boat ligand conformation for Ni(II) complex. The Cu(II) complex shows a 1:1 mononuclear structure with a square planar coordination polyhedron consisting of a L ligand and a highly non-symmetrical bonded acetate anion. Such a structural arrangement is dominated by the preferred coordination geometry of Cu(II) ion. The Zn(II) complex has two types of dimer structures with pairs of ZnL units bridged by two acetates in three different coordination modes. Consequently, both five-fold in trigonal bipyramidal and six-fold in octahedral coordination environments are present within one compound, which is a rare observation. The formation of ligand and the corresponding metal complexes has been confirmed by HR-ESI-MS, SEM-EDS and Raman spectroscopy. In addition, the complexation of HL with 3d metal ions results in slightly red shifts of the absorption maxima. As expected, the presence of Mn(II), Co(II)/Co(III), Ni(II) and Cu(II) ions quenches the ligand fluorescence emissions to some extent whilst the presence of Zn(II) has shown ligand fluorescence enhancement with the emission maximum further red-shift. Further studies on different anions and rare earth metal ions with such ligand are ongoing and will be reported in due course.

## Acknowledgements

DJF acknowledges Western Sydney University Postgraduate Research Award and LL thanks the receipt of an Australian Postgraduate Award and Western Sydney University Top-up Award; NDS thanks AINSE for an Honors Award. The crystallographic data collections for complexes 1-5 were undertaken on the MX1 beamline at the Australian Synchrotron, Victoria, Australia, through a collaborative access program (AS143MXCAP8503).

## References

- (a) A. W. Czarnik, *Acc. Chem. Res.* 1994, **27**, 302; (b) A. P. de Silva, H. Q. N. Gunaratne, T. Gunnlaugsson, A. J. M. Huxley, C. P. McCoy, J. T. Rademacher, T. E. Rice, *Chem. Rev.* 1997, **97**, 1515; (c) S. K. Sahoo, D. Sharma, R. K. Bera, G. Crisponi, J. F. Callen, *Chem. Soc. Rev.* 2012, **41**, 7195; (d) M. Wuttig, N. Yamada, *Nat. Mater.* 2007, **6**, 824; (e) M. Fernandez-Suarez, A. Y. Ting, *Nat. Rev. Mol. Cell. Biol.* 2008, **9**, 929; (f) G. Wu, F. Kong, J. Li, W. Chen, C. Zhang, Q. Chen, X. Zhang, S. Dai, *Synthetic Met.* 2013, **180**, 9; (g) H. Choi, J. K. Lee, K. H. Song, K. Song, S. O. Kang, J. Ko, *Tetrahedron*, 2007, **63**, 1553; (h) G. Wu, F. Kong, J. Li, X. Fang, Y. Li, S. Dai, Q. Chen, X. Zhang, *J. Power Sources*, 2013, **243**, 131; (i) M. A. Haidekker, T. Ling, M. Anglo, H. Y. Stevens, J. A. Frangos, E. A. Theodorakis, *Chem. Biol.* 2001, **8**, 123; (j) M. Horie, T. Sassa, D. Hashizume, Y. Suzuki, K. Osakada, T. Wada, *Angew. Chem. Int. Ed.* 2007, **46**, 4983.
- (a) J.-M. Lehn, *Supramolecular chemistry*, VCH, Weinheim, 1995; (b) J. W. Steed, D. R. Turner, K. J. Wallace, *Core concepts in supramolecular chemistry and nanochemistry*, John Wiley & Sons, Hoboken, 2007; (c) Z. Yang, J. Cao, Y. He, J. H. Yang, T. Kim, X. Peng, J. S. Kim, *Chem. Soc. Rev.* 2014, **43**, 4563.
- (a) Z. Dinev, J. N. Lambert, *Aust. J. Chem.* 2001, **54**, 625; (b) L. J. Beeching, C. S. Hawes, D. R. Turner, S. R. Batten, *CrystEngComm*. 2014, **16**, 6459; (c) T. W. Bell, N. M. Hext, *Chem. Soc. Rev.* 2004, **33**, 589.
- (a) J.-M. Lehn, *Science*, 2002, **295**, 2400; (b) W. Jiang, C. A. Schalley, *Proc. Natl. Acad. Sci.* 2008, **106**, 10425; (c) D. J. Cram, *Angew. Chem. Int. Ed.* 1986, **25**, 1039.
- (a) J. M. Kauffman, S. J. Imbesi, M. A. Aziz, *Org. Prep. Proced. Int.* 2001, **33**, 603; (b) J. J. Holt, B. D. Calitree, J. Vincek, M. K. Gannon, M. R. Detty, *J. Org. Chem.* 2007, **72**, 2690; (c) P. A. S. Smith, T.-Y. Yu, *J. Org. Chem.* 1952, **17**, 1281.
- (a) D. Maity, A. K. Manna, D. Karthigeyan, T. K. Kundu, S. K. Pati, T. Govindaraju, *Chem. Eur. J.* 2011, **17**, 11152; (b) K. B. Kim, G. J. Park, H. Kim, E. J. Song, J. M. Bae, C. Kim, *Inorg. Chem. Commun.* 2014, **46**, 237; (c) Y. J. Na, I. H. Hwang, H. Y. Jo, S. A. Lee, G. J. Park, C. Kim, *Inorg. Chem. Commun.* 2013, **35**, 342; (d) J. Jun Lee, G. Jin Park, Y. Sung Kim, S. Young Lee, H. Ji Lee, I. Noh, C. Kim, *Biosens. Bioelectron.* 2015, **69**, 226.
- (a) T. G. Jo, Y. J. Na, J. J. Lee, M. M. Lee, S. Y. Lee, C. Kim, *New J. Chem.* 2015, **39**, 2580; (b) J. H. Lee, S. H. Lee, Y. A. So, G. J. Park, C. Kim, *B. Korean Chem. Soc.* 2015, **36**, 1618; (c) T. G. Jo, Y. J. Na, J. J. Lee, M. M. Lee, S. Y. Lee, C. Kim, *Sensor. Actuat. B-Chem.* 2015, **211**, 498.
- (a) Y. S. Kim, G. J. Park, J. J. Lee, S. Y. Lee, S. Y. Lee, C. Kim, *RSC Adv.* 2015, **5**, 11229; (b) S. A. Lee, G. R. You, Y. W. Choi, H. Y. Jo, A. R. Kim, I. Noh, S.-J. Kim, Y. Kim, C. Kim, *Dalton Trans.* 2014, **43**, 6650; (c) G. J. Park, I. H. Hwang, E. J. Song, H. Kim, C. Kim, *Tetrahedron*, 2014, **70**, 2822.
- J. Y. Noh, S. Kim, I. H. Hwang, G. Y. Lee, J. Kang, S. H. Kim, J. Min, S. Park, C. Kim, J. Kim, *Dyes Pigments*, 2013, **99**, 1016.
- (a) G. J. Park, D. Y. Park, K.-M. Park, Y. Kim, S.-J. Kim, P.-S. Chang, C. Kim, *Tetrahedron*, 2014, **70**, 7429. (b) J. Yang, Z.-L. Yuan, G.-Q. Yu, S.-L. He, Q.-H. Wu, B. Jiang and G. Wei, *J. Fluoresc.* 2015, in press, Doi: 10.1007/s10895-015-1710-2.
- G. J. Park, Y. J. Na, H. Y. Jo, S. A. Lee, C. Kim, *Dalton Trans.* 2014, **43**, 6618.
- T. M. McPhillips, S. E. McPhillips, H. J. Chiu, A. E. Cohen, A. M. Deacon, P. J. Ellis, E. Garman, A. Gonzalez, N. K. Sauter, R. P. Phizackerley, S. M. Soltis, P. Kuhn, *J. Synchrotron Rad.* 2002, **9**, 401.
- W. Kabsch, *J. Appl. Crystallogr.* 1993, **26**, 795.
- G. M. Sheldrick, SADABS: Empirical Absorption and Correction Software, University of Göttingen, Germany, 1996.
- (a) G. M. Sheldrick, *Acta Crystallogr.* 2008, **A64**, 112; (b) G. M. Sheldrick, *Acta Cryst.* 2015, **A71**, 3.
- O. V. Dolomanov, L. J. Bourhis, R. J. Gildea, J. A. K. Howard, H. Puschmann, *J. Appl. Crystallogr.* 2009, **42**, 339.
- A. L. Spek, *Acta Crystallogr.* 2009, **D65**, 148.
- (a) S. Meghdadi, M. Amirnasr, S. B. Hoda Moein Sadat, K. Mereiter, A. Amiri, *Monatsh. Chem.* 2014, **145**, 1583; (b) D. W. Boyce, D. J. Salmon, W. B. Tolman, *Inorg. Chem.* 2014, **53**, 5788; (c) V. M. Manikandamathavan, T. Weyhermuller, R. P. Parameswari, M. Sathishkumar, V. Subramanian, B. U. Nair, *Dalton Trans.* 2014, **43**, 13018; (d) D. C. Sauer, H. Wadepohl, *Polyhedron*, 2014, **81**, 180.
- (a) A. Tissot, P. Fertey, R. Guillot, V. Briois, M.-L. Boillot, *Eur. J. Inorg. Chem.* 2014, 101; (b) K. A. Gerling, N. M. Rezayee, A. L. Rheingold, D. B. Green, J. M. Fritsch, *Dalton Trans.* 2014, **43**, 16498; (c) E. A. Buvaylo, V. N. Kokozay, K. Rubini, O. Yu. Vassilyeva, B. W. Skelton, *J. Mol. Struct.* 2014, **1072**, 129; (d) B. K. Koo, J. Korean Chem. Soc. 2013, **57**, 859; (e) Q.-Q. Zhang, Z.-H. Zhang, B.-H. Qu, Q. Chen, M.-Y. He, *Inorg. Chim. Acta*, 2014, **418**, 59; (f) P. Singh, D. P. Singh, V. P. Singh, *Polyhedron*, 2014, **81**, 56; (g) K. D. Murnaghan, C. Carbonera, L. Toupet, M. Griffin, M. M. Dirtu, C. Desplanches, Y. Garcia, E. Collet, J.-F. Letard, G. G. Morgan, *Chem. -Eur. J.* 2014, **20**, 5613; (h) D. Gong, B. Wang, X. Jia, X. Zhang, *Dalton Trans.* 2014, **43**, 4169.
- (a) G. Socrates, *Infrared and Raman Characteristic Group Frequencies: Tables and Charts*, 3rd ed. New York: John Wiley & Sons Hoboken, 2004; (b) V. Arjunan, S. Mohan, P. S. Balamourougane, P. Ravindran, *Spectrochimica Acta Part A*, 2009, **74**, 1215; (c) A. E. Ozel, S. Celik, S. Akyuz, *J. Mol. Struct.* 2009, **924–926**, 523.
- (a) Z. Xu, J. Yoon, D. R. Spring, *Chem. Soc. Rev.* 2010, **39**, 1996; (b) L. Fabbrizzi, M. Licchelli, P. Pallavicini, D. Sacchi, A. Taglietti, *Analyst*, 1996, **121**, 1763.

**TOC:** Five new complexes of a julolidine-quinoline based ligand with 3d transition metals featuring three monomers with metal to ligand ratios of 1:1 or 1:2, and two dimers bridged by acetate or methanol have been synthesised and structurally characterised.

